J. Earth Syst. Sci. (2020)129 36
https://doi.org/10.1007/s12040-019-1307-2

GIS based 3D visualization of subsurface geology and mapping of probable hydrocarbon locales, part of Cauvery Basin, India

J Saravanavel*, S M Ramasamy, K Palanivel and C J Kumanan

Department of Remote Sensing, Bharathidasan University, Tiruchirappalli, Tamil Nadu, India.
**Corresponding author. e-mail: drsaraj@gmail.com*

MS received 29 August 2018; revised 27 September 2019; accepted 4 October 2019

The hydrocarbon explorations were mostly guided by conventional geological and geophysical techniques in the past and modern tools like Remote Sensing, GIS, geophysical tomography came into being only during the last 2–3 decades. However, advanced virtues available with GIS, which could provide potential clues in deciphering the deep-seated natural resources were not capitalised deservingly. In this connection, the present article is the outcome of a study carried out in parts of Cauvery Basin, India for deciphering the subsurface hydrocarbon locales using Digital Elevation Modelling (DEM) techniques. The study was accomplished by the following hierarchical steps. (i) In the first step, DEM of gravity, litho tops depth of layered sedimentary rocks of Tertiary period and iso-resistivity data of 50 m depth were generated using Arc-GIS. (ii) It was followed by mapping the surface expressed circular features and the faults. (iii) Then, all the above surface and multi-depth data on the geological structures were integrated using Arc-GIS. (iv) From such an integration, 3D visualised domal structures of probable of hydrocarbon parentage were identified. (v) Finally, these were validated using known oil/gas wells. The study revealed the occurrence of domal structures with encircling peripheral faults from the subsurface to surface level in number of places. The spatial correlation of the known oil and gas occurrences with these 3D visualised domal structures indicated that the peripheral faults and domes have acted respectively as the zones of mobilisation and accumulation of oil and gas.

Keywords. Multi-depth DEM; 3D visualisation of subsurface geology; identification of hydrocarbon locales; Cauvery Basin, India.

1. Introduction

The faster depletion of fossil fuel caused the dire needs for locating newer hydrocarbon reservoirs all over the world. In the past, the conventional geological mapping, geophysical surveys, drilling and geochemical explorations dominantly guided the hydrocarbon explorations (Raiverman *et al.* 1966; Meijerink 1971; Balakrishnan and Sharma 1981; Biswas and Deshpande 1983; Kumar 1983; Mitra and Agarwal 1991; Prabhakar and Zutshi 1993; Rangaraju *et al.* 1993; Biswas 1998; Abrams 2005; Raum *et al.* 2005; Vishnu Vardhan *et al.* 2008; Kalpana *et al.* 2010). But of late, during the past 2–3 decades, many modern tools and technologies like Remote sensing, GIS, geophysical tomography and geochemistry have started finding more place in hydrocarbon prospecting (Van der Meer *et al.* 2000; Kumar *et al.* 2003, 2006; Banerjee and Mitra 2004; Vishnu Vardhan *et al.*

Published online: 20 December 2019

2004, 2008; Fainstein *et al.* 2008; Nicolas Pinet *et al.* 2008; Xuefeng Liu *et al.* 2008; Zhang *et al.* 2009, 2011; Arafat Mohmmed *et al.* 2011; Ana *et al.* 2012; Karim Allek *et al.* 2016; Mohammed Yasin *et al.* 2016). But, some of the virtues available with modern technologies are yet to be capitalised deservingly. For example, the DEM based 3D visualisation of subsurface geological structures, which can aid in narrowing down the target areas in the vast regions of hydrocarbon parentage, has not been attempted.

So, the present study was carried out in parts of Cauvery basin, Tamil Nadu, India (figure 1). This study is the demonstration of a new technique of DEM based 3D visualisation of subsurface geological structures related to hydrocarbon locales.

2. Geology and rationale of site selection

The study area exposes the rocks from oldest Precambrian crystalline to youngest Quaternary alluvium. The crystalline rocks are overlain by the successive younger layered rocks viz. clays and sandstones of Gondwana Group; limestone, shales and sandstones of Cretaceous Group; and sandstones and laterites of Lower Miocene, Middle–Upper Miocene and Pliocene rocks/formations of Tertiary Group (figure 1). While, the Precambrian crystalline rocks form the basement, the overlying layered sequence of rocks from Gondwana to Tertiary periods show easterly dip at low angles of 5°–10° towards the east coast of Tamil Nadu. Thus, the rock types exhibit a picture of a

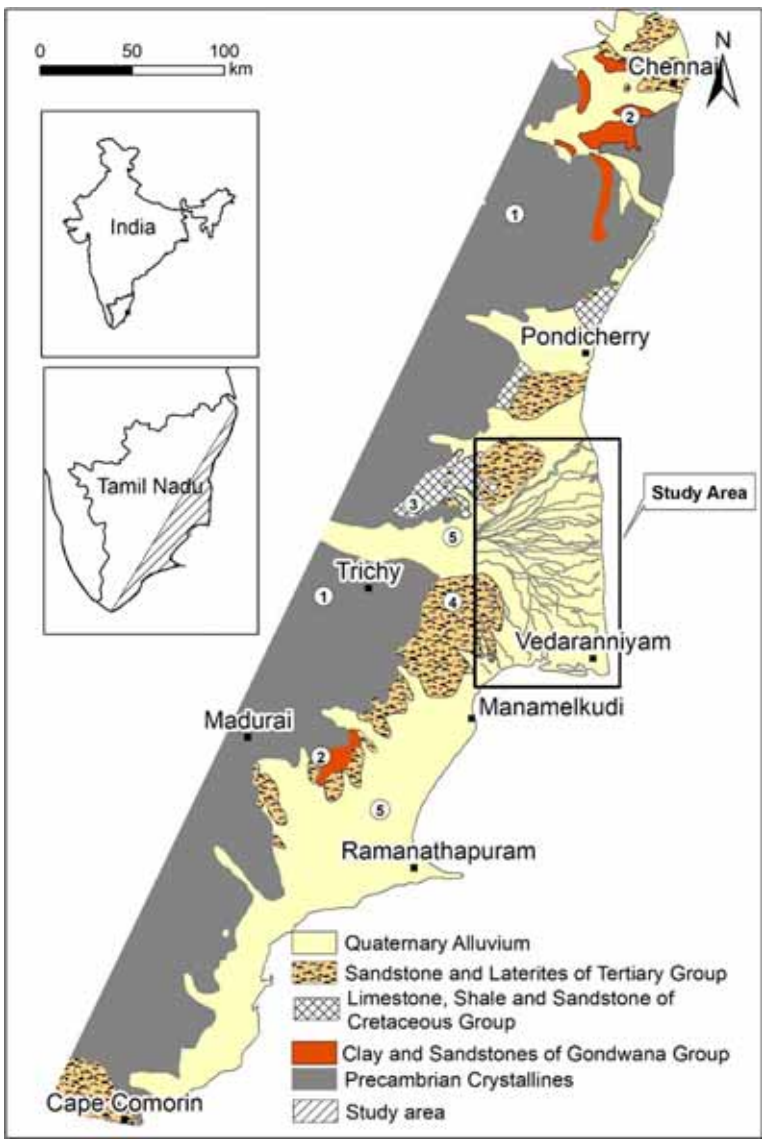

Figure 1. Geology of the study region. The older Precambrian crystalines are overlained by the layered younger sedimentary rocks with low easterly dip towards the coast providing a scenario of slided pack of cards.

slided pack of cards with oldest crystallines/ Gondwanas in the west and younger layered rocks successively towards easterly. The Quaternary alluvium covers all these rocks either partly or fully. So, the study sector covering an area of 7800 km^2 was selected in the eastern part of Cauvery delta, where such layered sequence of rocks occurs from the surface to subsurface.

The basement crystalline and the overlying layered sequence of rocks of Gondwana–Tertiary groups (figure 1) thus provided the possibility for GIS based 3D visualisation of multi-depth geological data. The availability of adequate borehole lithology drilled by the Oil and Natural Gas Commission, Govt. of India (Anon 1973) and also the gravity data (Anon 2000) provided further credentials for selecting the study area for the present 3D visualisation of subsurface geological structures of hydrocarbon parentage.

3. Methodology

In the study, Bouger gravity contour data was collected from seismo-tectonic atlas (Anon 2000) and geo-referenced. It was given as input in Arc-GIS and utilising the 'Contour to Digital Elevation Model tool' of the '3D Analyst Module', Digital Elevation Model was developed from the gravity contours (figure 2). The gravity DEM generated, thus displayed the gravity contour values in the form of 3D landscape. Such landscape showed the zones of higher gravity values as elliptical and circular domes, peaks and plateaux and the lower gravity values as basins/linear depressions (figure 2). From the gravity DEM, gravity domes/peaks/plateaux were interpreted as highs or structural domes, whereas the linear depressions and breaks in slopes were mapped as faults of the basement rocks (figure 2). Similarly, the litholog data from the Quaternaries on the top to Tertiaries in the bottom, were collected from 55 boreholes (figure 3a) drilled by the Oil and Natural Gas Commission, Government of India (Anon 1973). From these lithologs, the depths at which the contacts between various rocks of Tertiary period were identified. For example, the contacts between (i) Lower Miocene and Middle–Upper Miocene, (ii) Middle–Upper Miocene and Pliocene and (iii) Pliocene and Quaternaries were identified (figure 3b). Such measured depths of the lithological contacts of various Tertiary rocks were respectively considered as the top surfaces or litho

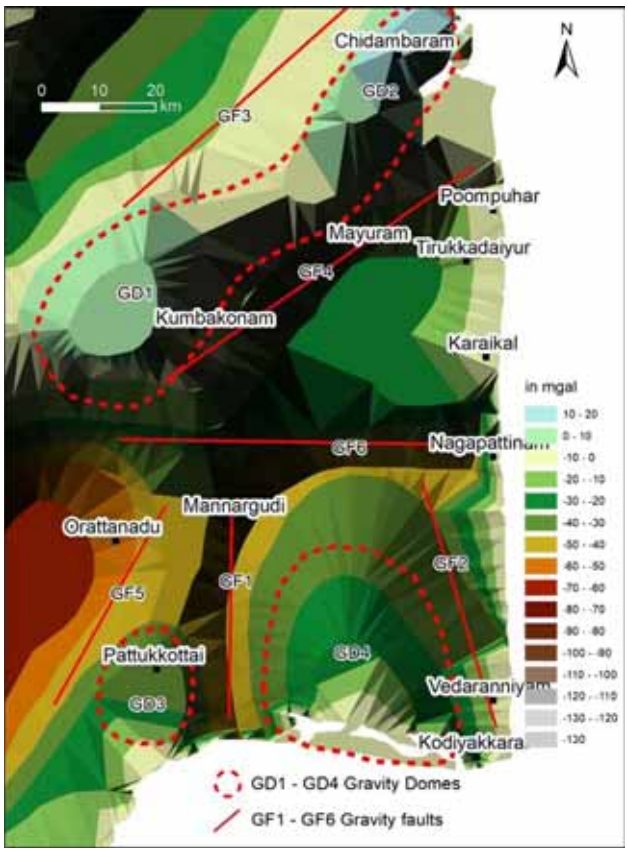

Figure 2. Digital Elevation Model of Bouger gravity data showing the possible domes and faults of the basement crystalline.

tops of these three Tertiary formations/rocks, namely the Lower Miocene, Middle–Upper Miocene and Pliocene.

These litho top values of the three formations encountered in the 55 boreholes were independently entered in Arc-GIS software with longitudes and latitudes respectively as 'X' and 'Y' and the litho tops of Lower Miocene, Middle–Upper Miocene and Pliocene rocks respectively as Z1, Z2 and Z3 values. From these, three independent DEMs were generated for these litho tops using 'Point to DEM tool' of the '3D Analyst Module' of Arc-GIS. In these Digital Elevation Models, the litho tops occurring at shallow depths with reference to ground level have appeared as deeps/basins due to lower numerical values. In contrast, the litho tops occurring at deeper depths have appeared as domes/peaks, again owing to the higher numerical values. Thus, the DEM exhibited inverse topography of the litho tops. So, in order to have the actual topographic representation of the litho tops of these formations, these three DEM's were inverted using the provisions available in Arc-GIS (figures 4–6). From these three inverted DEM's of

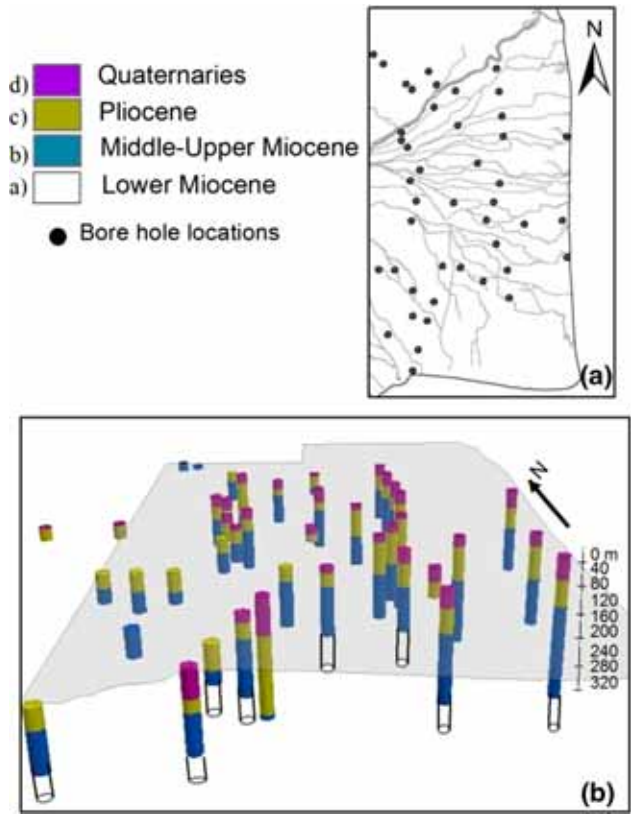

Figure 3. (**a**) Locations of boreholes of the study area; (**b**) (1) Lower Miocene, (2) Middle–Upper Miocene, (3) Pliocene, and (4) Quaternary sediments interpreted from lithologs of the borehole.

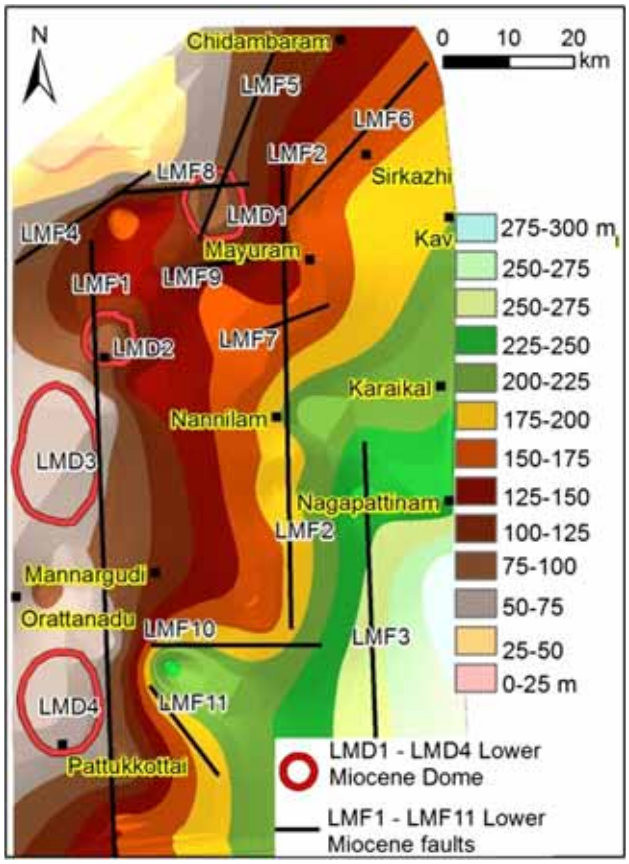

Figure 4. Digital Elevation Model of the top surface (litho top) of Lower Miocene formation and the interpreted domes (LMD1–LMD4) and faults (LMF1–LMF11).

the litho tops of Lower Miocene, Middle–Upper Miocene and Pliocene formations/rocks, the elevated circular and elliptical zones were marked as domes and the linear depressions as faults.

Similarly, the apparent resistivity values collected for 50 m depth from 250 geophysical resistivity depth probe points (figure 7) were given as inputs in Arc-GIS and the resistivity DEM was generated. In this case, 'Contour to DEM tool' of Arc-GIS was used again to prepare the DEM, as was done in the case of gravity data. In this case, the DEM has displayed the zones of low resistivity values as basins/linear depressions and that of the higher values as domes/peaks, respectively, due to the lower and higher apparent resistivity values. So, the DEM was kept as such without inverting it. From such resistivity DEM, the zones of resistivity peaks and highs were marked as domes and the linear depressions/valleys as faults at 50 m depth (figure 7). Then the enlarged formats of IRS FCC satellite data were interpreted and ring/circular features and the lineaments were interpreted to start with and the active faults were subsequently interpreted from drainage and geomorphic anomalies (figure 8). Finally, all these domes and faults interpreted from basement to top, from (i) gravity data, (ii) litho top data of three Tertiary formations, (iii) resistivity data of 50 m depth and (iv) ring/circular features and active faults interpreted at the surface level from IRS FCC satellite data were integrated using Arc-GIS (figure 9). From such integration, the zones of coincidence of domes and the lineaments/faults were mapped respectively as growth domes and growth faults. These growth features were three dimensionally visualized and elucidated for their hydrocarbon potentials using the known oil/gas wells (figures 10 and 11).

4. 3D visualization of subsurface geology

4.1 *Gravity DEM and geological structures*

The Bouger gravity values of the study area varied from +10 mgal to −13 mgal. The Arc-GIS has considered the −13 mgal as the lowest and +10 mgal as the highest values and it generated

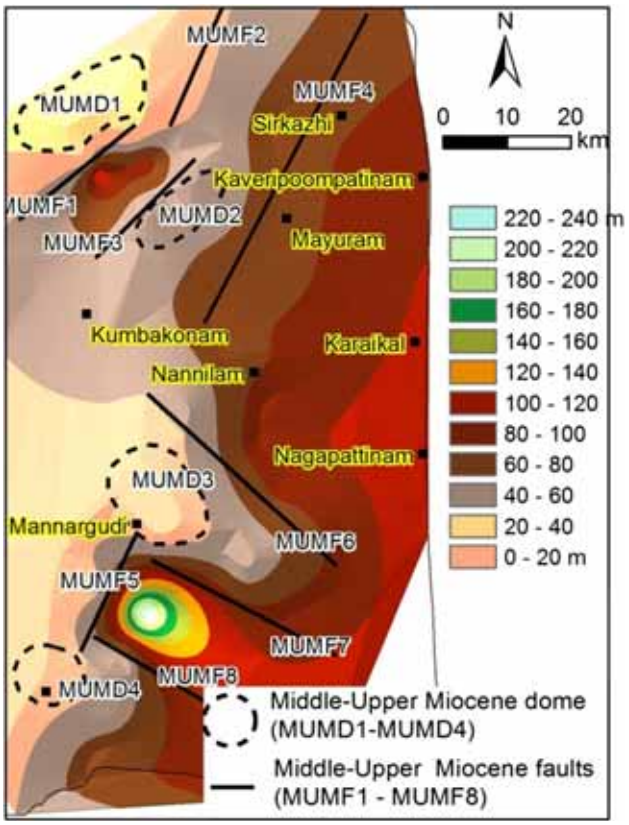

Figure 5. Digital Elevation Model of the top surface (litho top) of Middle–Upper Miocene formation and the interpreted domes (MUMD1–MUMD4) and faults (MUMF1–MUMF8).

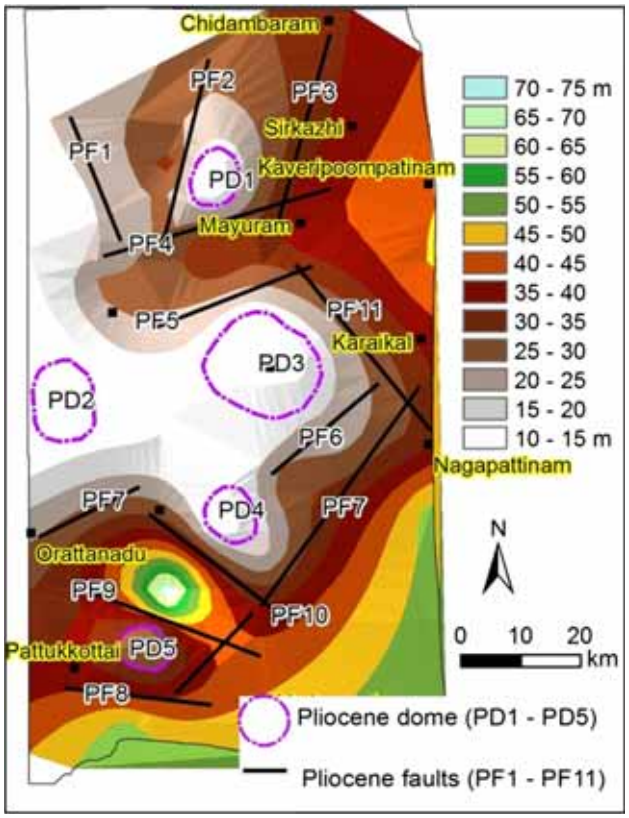

Figure 6. Digital Elevation Model of the top surface (litho top) of Pliocene formation and the interpreted domes (PD1–PD5) and faults (PF1–PF11).

DEM keeping this range at 23 levels in this case. From gravity DEM, three circular and elliptical domes were interpreted as gravity/basement domes (BD1–BD3) and six linear gravity depressions and breaks in slopes as gravity faults (BF1–BF6, figure 3).

4.2 *Litho top DEM and geological structures*

The inverted DEM generated for the litho tops of Lower Miocene, Middle–Upper Miocene and Pliocene formations of the Tertiary group (figure 3) were interpreted and independent GIS databases were generated showing the domes and the faults seen on the top surfaces of these three Tertiary formations (figures 4–6). From Lower Miocene litho top DEM, four circular and elliptical peaks and plateaux were interpreted and termed as LMD1–LMD4 (Lower Miocene domes). Similarly, the eleven linear depressions and breaks in slopes were interpreted as LMF1–LMF11 (Lower Miocene faults) (figure 4). From the Middle–Upper Miocene litho top DEM, four Middle–Upper Miocene domes (MUMD1–MUMD4) and faults (MUMF1–MUMF4) were interpreted (figure 5). In the same way, from the Pliocene litho top DEM, five Pliocene domes (PD1–PD5) and 11 Pliocene faults (PF1–PF11) were interpreted (figure 6).

4.3 *Resistivity DEM and geological structures*

From the resistivity DEM of 50 m depth, 12 resistivity domes (RD1–RD12) and 18 resistivity faults (RF1–RF18) were interpreted (figure 7). In this case, again, the zones of resistivity peaks, elliptical highs and plateaux were interpreted as resistivity domes and breaks in slopes and well defined linear resistivity lows as resistivity faults.

4.4 *Surface domes and faults*

Various earlier workers have used different drainage anomalies like annular, curvilinear and radial centripetal drainages to decipher and map the surficial and subsurface domal structures using topographic data, aerial photographs and satellite data (Whitehouse 1941; King 1942; Isachsen 1975; Twidale 2004; Stewart 2015). Similarly, the linear

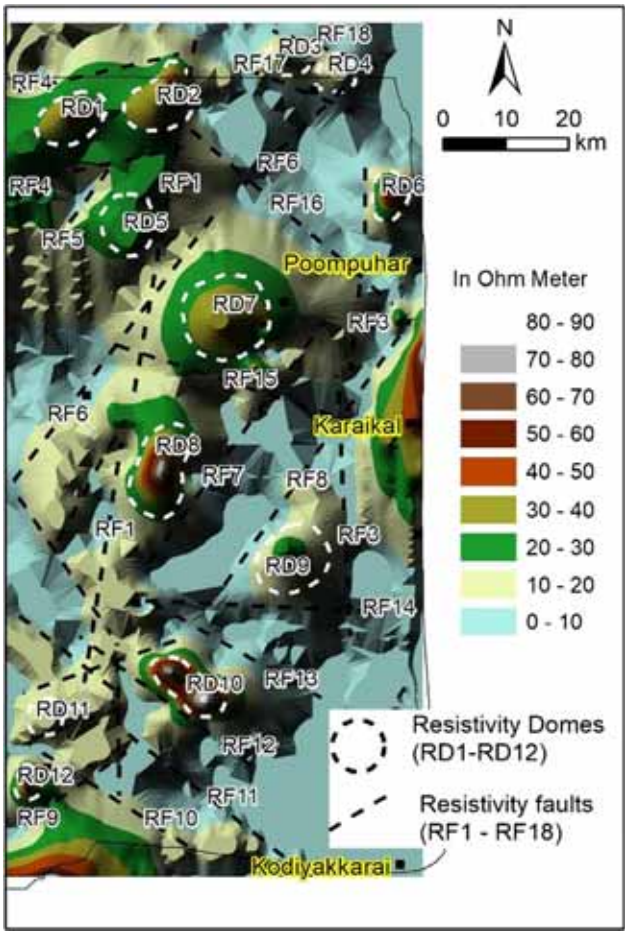

Figure 7. Digital Elevation Model of the geophysical resistivity values of 50 m depth and interpreted resistivity domes (RD1–RD12) and faults (RF1–RF18).

and deflected drainages, eyed drainages, compressed meanders with 'Z' and 'S' shaped drags were used as guides to detect active faults by many researchers (Thornbury 1985; Smith *et al.* 1997; Valdiya 2001; Twidale 2004; Jain and Sinha 2005; Ramasamy 2006; Ramasamy *et al.* 2006, 2011; Mrinalinee Devi *et al.* 2011). Further, several researchers have observed that the circular features seen in satellite images and aerial photographs at the surface have coincided with subsurface oil bearing structures in parts of Cauvery delta (Babu 1975; Mitra and Agarwal 1991; Ramasamy *et al.* 2006).

So, interpretations were made using the topographic sheets and IRS satellite data to map specifically the circular features and the lineaments/active faults in the study area from various photo recognition elements and drainage anomalies. Based on annular drainages seen in the area, 18 circular features were interpreted as shown in figure 8(a and b). The drainages have also exhibited major abrupt deflections in nine locations similar to one shown in figure 8(c) and these were interpreted as deflected drainages and the lineaments that have caused such deflections were interpreted as active faults. The river Coleroon, north of Sirkazhi (figure 8d) and many such distributaries of Cauvery river showed eyed drainages in the study area. From it, the lineaments bisecting such eyed drainages were interpreted as active faults, because these faults only have caused land subsidence and the resultant split up of the channels as observed by Smith *et al.* (1997) in Panhandle region of Botswana. Ramasamy and Karthikeyan (1998), Ramasamy and Kumanan (2000) and Ramasamy *et al.* (2011) have also made similar observations from different parts of South India. Further, the eyed drainage in river Coleroon in the area north of Sirkazhi (figure 8d) showed 'S' shaped drag. This indicates sinistral movements along a N–S lineament/fault which is bisecting it. Whereas, from the broad 'Z' shaped drag observed in the eyed drainage in Coleroon river near Thanjavur, dextral movement was inferred along the bisecting of NW–SE lineament/fault (figure 8e). The bundles of distributary channels of Cauvery river seen to the west of Kumbakonam (figure 8f) showed acute compressed meandering with 'S' shaped drags within two N–S faults. This led to the inference of sinistral couple along the two N–S faults. Whereas the large number of 'Z' shaped compressed meanders seen in IRS satellite data in an area of 150 km^2 around Nannilam, and confined within two NW–SE trending sub-parallel lineaments, suggest the possible dextral movements along these two lineaments/faults (figure 8g). Thus, circular features and active faults were interpreted from various drainage anomalies observed in the satellite data (figure 8).

4.5 *3D Visualisation of subsurface geological structures*

All such domes and faults interpreted at the surface and multiple depths from (i) gravity, (ii) litho tops of Lower Miocene, (iii) Middle–Upper Miocene and (iv) Pliocene formations, (v) apparent resistivity of 50 m depth, and (vi) satellite imagery data were integrated using the overlay function of Arc-GIS and an integrated map was prepared showing all the multi-depth tectonic features. Such integration showed that, the domes and faults inferred at multiple depths and in different layered

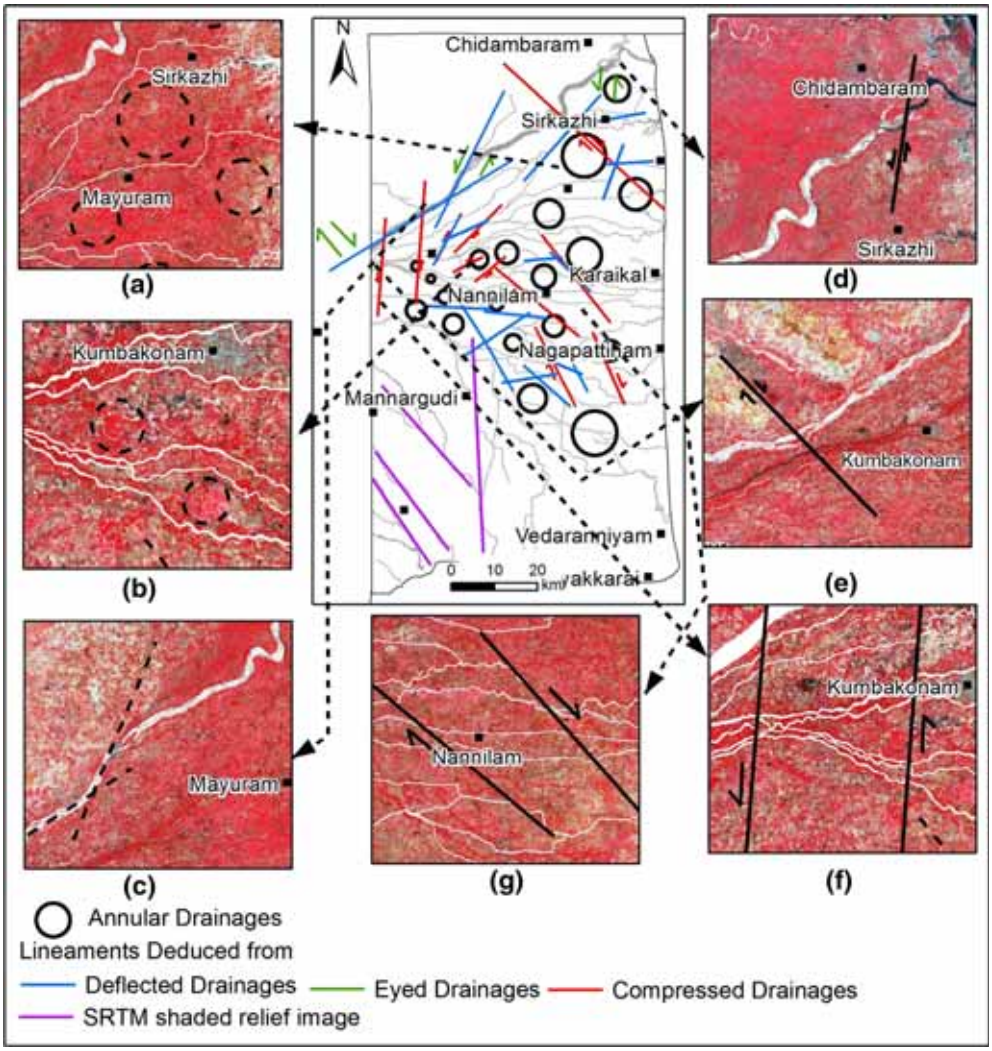

Figure 8. Surface domes and faults, Cauvery delta. IRS satellite FCC images showing annular and curvilinear drainages and circular features (**a**, **b**), deflected Coleroon river and NE–SW/NNE–SSW lineaments (**c**), eyed drainages with 'S' shaped drags and N–S sinistral faults (**d**), eyed drainage with 'Z' shaped drags and NW–SE dextral fault (**e**), 'S' shaped compressed drainages and N–S sinistral faults (**f**), 'Z' shaped compressed drainages and NW–SE dextral faults (**g**).

sedimentary formations have coincided with each other in several parts of the study area and thus formed clusters in the integrated map (figure 9). Overall, seven such clusters of multi-depth domes and faults were found in the study area (A–G, figure 9). In such clusters, domes were found in the centre and faults were encircling the domes along their peripheries. These seven clusters of domes and the corresponding faults were studied individually. The cluster A and C, studied thus, are shown respectively in figure 10(a and b), as example. These two clusters revealed that in both cases, the domes and peripheral faults were found in almost all depths from the lower older to the upper younger rock types viz. crystalline basement, Lower Miocene, Middle–Upper Miocene, Pliocene, at 50 m depth resistivity data and the Quaternaries.

Such multi-depth data stacked for three dimensionally visualising the structures for cluster A is shown in figure 11 as example. It showed that in the older Tertiary rocks of Lower Miocene age, the dome was wider and the same has gradually become smaller in the successive overlying younger rocks of Middle–Upper Miocene and Pliocene age, and in the top Quaternary formations (figure 11). Similarly, the gaps in between the peripheral faults were wider in the older basement crystalline and gradually reduced in the upper younger rock types (figures 10 and 11). Though this pattern is generally seen in the area, in some clusters, the circumferences of the domes in the lower older rock

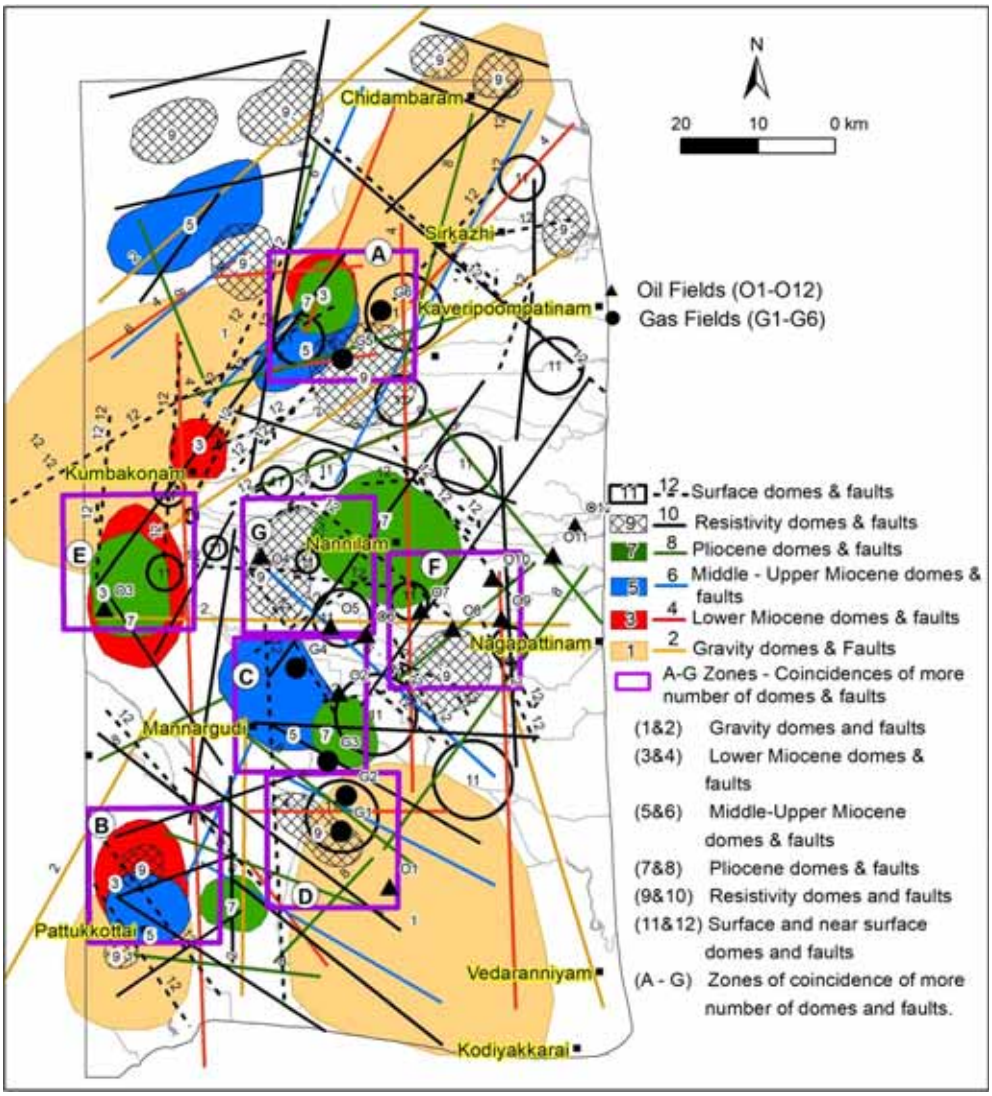

Figure 9. Multi-depth and surface tectonic features.

types were less and the upper younger rock types were more, thus appearing like mushrooms. Further, the peripheral faults also correspondingly varied in their gaps according to the morphology of the domes.

5. Discussions

In the study, clusters of multi-depth domes and faults were found in seven locations in the study area (figure 9). The 3D visualisation of these structures (figures 10 and 11) shows that the domes and the faults continue from the Precambrian basement, right through the overlying sequence of Tertiary rocks and the Quaternaries at the surface (figures 2–10). This indicates that the clusters of domes and faults might have been formed due to the Post Tertiary/Quaternary deformations. Ramsay (1967) observed that domes and basins are possible in a single deformation itself. So, such post Tertiary or Quaternary deformation would have caused such domes and basins. These types of tectonic features were found by several earlier workers in parts of South India, including the Cauvery delta (Raiverman *et al.* 1966; Balakrishnan and Sharma 1981; Kumar 1983; Mitra and Agarwal 1991; Rangaraju *et al.* 1993; Sahu *et al.* 1995). While Subrahmanya (1996) inferred the possibility of active deformation in South India, Ramasamy (2006) developed a post-collision tectonic model for the whole of the Indian plate. In the said model, he demonstrated the following: (i) the northerly directed compressive

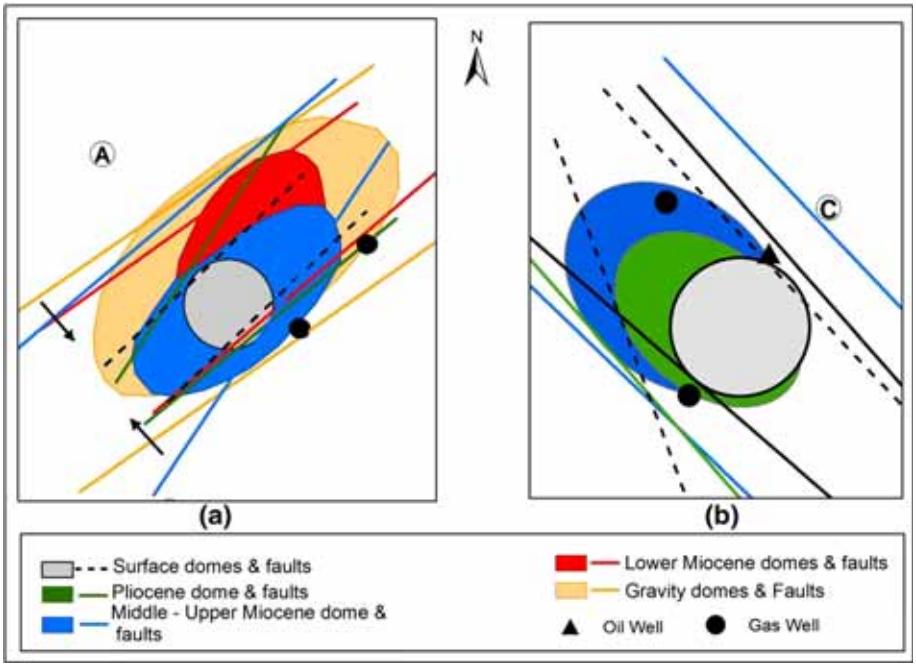

Figure 10. (**a**, **b**) Multi-depth domes and faults in clusters A and C.

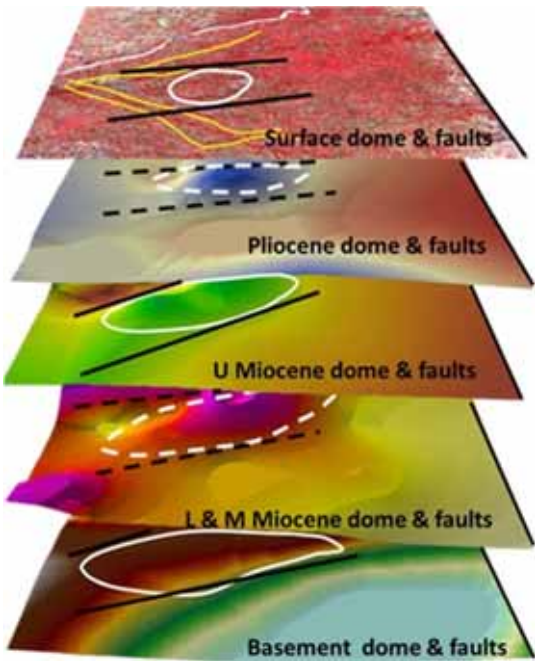

Figure 11. Three dimensionally visualized conceptual model on surface to subsurface domes and faults.

force, which has originally drifted the Indian plate towards northerly, made it to collide with Eurasian plate and resulted the rise of Himalayan Mountains, is still active. (ii) Such active force is pushing the Indian plate towards northerly even today. (iii) But, since the Himalayas obstructs from the north, this force is adjusted within the Indian Plate. (iv) Such adjustments are causing a series of east-west trending arches and complementary deeps and N–S extensional, NE–SW sinistral and NW–SE dextral faults in the whole of Indian plate. Ramasamy and Balaji (1996) observed that clusters of Precambrian domes and basins of parts of Tamil Nadu are confined within two sub-parallel sets of NE–SW and NW–SE transverse fault systems. From this, they have inferred that these domes and basins were formed due to the movements along these faults and called these domes and basins as faults followed folds.

In the present study area also, the clusters of domes are confined within NE–SW sinistral and NW–SE dextral faults related to post-collision tectonics demonstrated by Ramasamy (2006). These clusters of domes might have been formed due to the transverse movements along the above sets of faults as faults followed folds related to post-collision tectonic phenomenon. The continuity of the peripheral faults encircling the domes from Precambrian basement up to the top most Quaternaries shows that these faults might have acted as gliding surfaces. Along these surfaces, the rocks might have moved causing these clusters of domes. Further, the mushroom type of morphology of the domes in some of the clusters confirms not only the gliding but also the phenomenon of diaphirism. Again, since the domes of the younger rock types are coinciding with the basement domes of the

Precambrian period in some places, these basement domes might have provided positive topography, over which the domes of the younger rock types have formed during the post-collision tectonics of the Quaternary period.

The super position of the spatial data showing the 18 oil and gas wells of the study area (Chaudhuri *et al.* 2010) was done over the map showing the cluster of domesusing Arc-GIS (figures 9 and 10). The same revealed that the oil and gas fields mostly fell along the peripheral faults that are fringing the domes (figures 9 and 10). It follows from it that these peripheral faults might have acted as conduits for the migration of oil and gas from the deeper source rocks as well as acted as loci for the oil and gas accumulations.

6. Conclusions

Due to the depletion of existing fossil fuels, the need has emerged in all over the world to locate newer hydrocarbon reservoirs. At the same time, though there are a number of frontier basins covering thousands of sq. km in the Indian subcontinent, the scientists are yet relying on geophysical exploration, deep drilling and geochemical exploration only. This might not be possible to cover the vast frontier basins. At the same time, the remote sensing technology has emerged as a potential tool in identifying the active tectonic corridors and geomorphic mapping leading to the identification of target areas for hydrocarbon locales (Smith *et al.* 1997; Valdiya 2001; Twidale 2004; Jain and Sinha 2005; Ramasamy 2006; Ramasamy *et al.* 2006, 2011; Mrinalinee Devi *et al.* 2011). The GIS also possesses unique credentials in integration of large volume of multi-theme data and 3D visualisation. But still, the development of viable techniques for locating the deep seated hydrocarbon reservoirs are yet far away. In this context, the present study is a newer attempt made to interpret large volume of multi-theme data and three dimensionally visualise the subsurface geological structures using GIS technology. Such DEM based GIS technique developed in this study proved to be a potential tool in narrowing down the target areas in the vast frontier basins.

Acknowledgements

The authors acknowledge Oil Industry Development board (OIDB), New Delhi which has provided the stimuli for the present study. The authors also acknowledge the Bharathidasan University for facilitating the work.

References

Abrams M A 2005 Significance of hydrocarbon seepage relative to petroleum generation and entrapment; *Mar. Petrol. Geol.* **22** 457–477.

Ana P, Khan S D and Thurmond A K 2012 Integrated hyperspectral remote sensing, geochemical and isotopic studies for understanding hydrocarbon-induced rock alterations; *Mar. Petrol. Geol.* **35**(**1**) 292–308.

Anon 1973 UNDP project on groundwater investigation in Tamil Nadu, Tamil Nadu Public Works Department, unpublished technical report.

Anon 2000 GSI, 'Seismotectonic Atlas of India and Its Environs,' Geological Survey of India, Bangalore.

Arafat Mohmmed M, Palanivel K, Kumanan C J and Saravanavel J 2011 Geospatial mapping and 3D GIS based visualization of subsurface structures; *Inter. Geoinfor. Res. Devel. J.* **2(2)** 66–74.

Babu P V L P 1975 A study of cyclic erosion surfaces and sedimentary unconformities in the Cauvery basin, South India; *J. Geol. Soc. India* **16(3)** 349–353.

Balakrishnan T S and Sharma D S 1981 Tectonics of Cauvery Basin; *Bull. Oil Natural Gas Comm.* **18** 49–51.

Banerjee S and Mitra S 2004 Remote surface mapping using orthophotos and geologic maps draped over digital elevation models: Application to the Sheep Mountain anticline, Wyoming; *AAPG Bull.* **88(9)** 1227–1237.

Biswas S K 1998 Overview of sedimentary basins of India and their hydrocarbon resource potential, *Proc. Nat. Symp*: *Recent researches in sedimentary basins*, pp. 1–25.

Biswas S K and Deshpande S V 1983 Geology and hydrocarbon prospects of Kutch, Saurashtra and Narmada basins; *Petrol. Asia J.*, pp. 111–126.

Chaudhuri A, Rao M V, Dobriyal J P, Saha G C, Chidambaram L, Mehta A K, Ramana L V and Murthy K S 2010 Prospectivity of Cauvery Basin in deep syn-rift sequences, SE India, Search and Discovery Article #10232 (2010).

Fainstein R, Koeninger C, Banik N and Broetz R 2008 Sub-Basalt Mesozoic Imaging Offshore India, Abs. GEO India Expo XXI, Noida, New Delhi, India, AAPG Search and Discovery.

Isachsen Y W 1975 Possible evidence for contemporary doming of the Adirondack Mountains, New York, and suggested implications for regional tectonics and seismicity; *Tectonophys.* **29** 169–181.

Jain V and Sinha R 2005 Response of active tectonics on the alluvial Baghmati River, Himalayan foreland basin, eastern India; *Geomorphology* **70(3–4)** 339–356.

Kalpana M S, Patil D J, Dayal A M and Raju S V 2010 Near surface manifestation of hydrocarbons in Proterozoic Bhima and Kaladgi Basins implications to hydrocarbon resource potential; *J. Geol. Soc. India* **76** 548–556.

Karim A, Boubaya D, Bouguern A and Hamoudi M 2016 Spatial association analysis between hydrocarbon fields and sedimentary residual magnetic anomalies using Weights of

Evidence: An example from the Triassic Province of Algeria; *J. Appl. Geophys.* **135** 100–110.

King L C 1942 South African Scenery, Oliver and Boyd, Edinburgh, 340p.

Kumar B, Das Sharma S, Patil D J, Sreenivas B, Kalpana G, Smitha K Panicker, Vishnu Vardhan C and Raju S V 2003 Adsorbed soil gas surveys for hydrocarbon research and exploration in Kutch Onland Basin, Gujarat, NGRI Tech. Rep. No. 2003-Exp-400.

Kumar B, Raju S V, Patil D J, Kalpana G and Vishnu Vardhan C 2006 Integrating surface geochemical expressions with geological, geophysical and remote sensing data: case histories from selected Proterozoic Basins of India, extended abstract submitted at AAPG 2006 Annual Convention, held during April 9–12, 2006, Houston.

Kumar S P 1983 Geology and hydrocarbon prospects of Krishna, Godavari and Cauvery basins; *Petrol. Asia* **6(4)** 57–65.

Meijerink A M J 1971 Reconnaissance survey of the Quaternary Geology of the Cauvery Delta; *J. Geol. Soc. India* **12** 113–124.

Mitra D S and Agarwal R P 1991 Geomorphology and Petroleum prospects of Cauvery basin, Tamilnadu, based on interpretation of Indian Remote Sensing Satellite (IRS) data; *J. Indian Soc. Remote Sens.* **19(4)** 263–268.

Mohammedyasin S M, Lippard S J, Omosanya K O, Johansen S E and Harishidayat D 2016 Deep-seated faults and hydrocarbon leakage in the Snøhvit Gas Field, Hammerfest Basin, Southwestern Barents Sea; *Marine Petrol. Geol.* **77** 160–178.

Mrinalinee Devi R K, Bhakuni S S and Pabon Kumar Bora 2011 Tectonic implication of drainage set-up in the Sub-Himalaya: A case study of Papumpare district, Arunachal Himalaya, India; *Geomorphology* **127(1–2)** 14–31.

Nicolas P, Duchesne M, Lavoie D, Bolduc A and Long B 2008 Surface and subsurface signatures of gas seepage in the St. Lawrence Estuary (Canada): Significance to hydrocarbon exploration; *Marine Petrol. Geol.* **25(3)** 271–288.

Prabhakar K N and Zutshi P L 1993 Evolution of southern part of Indian east coast sedimentary basins; *J. Geol. Soc. India* **41(7)** 215–250.

Raiverman V, Singh G and Murti K V S 1966 Fracture Pattern in Cauvery basin; *Bull. Oil Nat. Gas Comm.* **3** 13–20.

Ramasamy S M 2006 Remote sensing and active tectonics of South India; *Inter. J. Remote Sens.*, Taylor and Francis, London **27(20)** 4397–4431.

Ramasamy S M and Balaji S 1996 Origin of Domes and basins in Precambrian fold belts of South India. *Proc. Vol. of National Seminar on Precambrian Geology*, Madras University, Chennai, pp. 68–70.

Ramasamy S M and Karthikeyan N 1998 Pleistocene/ Holocene Graben along Pondicherry—Cumbum Valley, Tamil Nadu, India; *Geocarto Inter.* **13(3)** 83–90.

Ramasamy S M and Kumanan C J 2000 Eyed drainages observed in IRS imagery in Tamil Nadu and their geological significance; *Inter. J. Remote Sens.* **21(3)** 475–481.

Ramasamy S M, Saravanavel J and Selvakumar R 2006 Late Holocene geomorphic Evolution of Cauvery delta, Tamil Nadu, India; *J. Geol. Soc. India* **67(5)** 649–657.

Ramasamy S M, Kumanan C J, Selvakumar R and Saravanavel J 2011 Drainage anomalies observed in IRS Satellite Imagery and their tectonic significance in South India; *Tectonophys.* **501** 41–51.

Ramsay J G 1967 *Folding and fracturing of rocks*; McGraw Hill book company, New York, 568p.

Rangaraju M K, Agarwal A and Prabhakar K N 1993 Tectono-stratigraphy, structural styles, evolutionary model and hydrocarbon habitat, Cauvery and Palar basins; In: *Proceedings of the 2nd Seminar on Petroliferous basins of India* (eds) Biswas S K, Alok Dave, Garg P, Jagadish Pandey, Maithani A and Thomas N J, Vol. 1, pp. 371–388.

Raum T, Mjelde R, Berge A M, Paulsen J T, Digranes P, Shimamura H, Shiobara H, Kodaira S, Larsen V B, Fredsted R, Harrison D J and Johnson M 2005 Sub-basalt structures east of the Faroe Islands revealed from wide-angle seismic and gravity data; *Petrol. Geosci.* **11(4)** 291–308.

Sahu J N, Banerjee B, Zutshi P L and Kuldeep Chandra 1995 Evolution of the Cauvery basin, India from subsidence modelling; *Marine Petrol. Geol.* **12(6)** 667–675.

Smith N D, McCarthy T S, Ellery W N, Merry C L and Ruther H 1997 Avulsion and anastomosis in the Panhandle region of the Kavango Fan, Botswana; *Geomorphology* **20(1–2)** 49–65.

Stewart S A 2015 Circular geological structures outcropping in the sedimentary basins of Saudi Arabia; *J. Asian Earth Sci.* **106** 95–118.

Subrahmanya K R 1996 Active intraplate deformation in South India; *Tectonophys.* **262** 231–241.

Thornbury 1985 *Principles of geomorphology*; 2nd Edition, John Wiley and sons inc., New York, 594p.

Twidale C R 2004 River patterns and their meaning; *Earth-Sci. Rev.* **67** 159–218.

Valdiya K S 2001 Tectonic resurgence of the Mysore Plateau and surrounding region in cratonic South India; *Curr. Sci.* **81(8)** 1068–1089.

Van der Meer F D, van Dijk P M, Schetselaar E M, Little M, Podlaha O, Yang Hong and Biegert E 2000 An integrated geoscience approach for hyperspectral hydrocarbon microseepage detection; In: *2000 Proceedings of the 15th international conference on applied geologic remote sensing*, Environmental Research Institute on Michigan (ERIM), pp. 81–88.

Vishnu Vardhan C, Kumar B, Kumanan C J, Devleena M and Patil D J 2008 Hydrocarbon prospects in Sub Trappean Mesozoic Deccan Syneclise Basin, India: Evidences from surface geochemical prospecting search and discovery; *AAPG Online Journal*.

Vishnu Vardhan C, Smitha K Panicker and Kumar B 2004 Comparison of Proterozoic basins of India with similar basins of the world: Implications to hydrocarbon resource prospects; In: *Proc. 6th International Conference on Geochemistry and Exploration in the Afro-Asian Region*, 12–14 October 2004, Beijing, China Pub., Taylor & Francis.

Whitehouse F W 1941 The surface of western Queensland, *Proc. Royal Soc. Queensland*, **53** 1–22.

Xuefeng L, Zhong G, Yin J, He Y and Li 2008 GIS-based modeling of secondary hydrocarbon migration pathways and its application in the northern Songliao Basin, northeast China; *Comput. Geosci.* **34(9)** 1115–1126.

Zhang G, Zou L, Shen X, Lu S, Li C and Chen H 2009 Remote sensing detection of heavy oil through spectral enhancement techniques in the western slope zone of Songliao Basin, China; *AAPG Bull.* **93(1)** 31–49.

Zhang G, Zheng Z, Shen X, Zou L and Huang K 2011 Remote sensing interpretation of areas with hydrocarbon microseepages in northeast China using Landsat-7/ETM+ data processing techniques; *Int. J. Remote Sens.* **32(21)** 6695–6711.

Corresponding editor: Santanu Banerjee